Arab J Sci Eng (2015) 40:1141–1150
DOI 10.1007/s13369-015-1573-5

RESEARCH ARTICLE - MECHANICAL ENGINEERING

Thermal Performance Studies on Multi-pass Flat-plate Solar Air Heater with Longitudinal Fins: An Analytical Approach

P. Velmurugan · R. Kalaivanan

Received: 24 July 2014 / Accepted: 19 January 2015 / Published online: 6 February 2015

Abstract In this study, thermal performance of double- and triple-pass solar air heater with longitudinal fins is mathematically evaluated. The effects of parameters, viz. mass flow rate, solar intensity and inlet temperature upon outlet temperature, thermal efficiency and increments in efficiency, power consumption are presented. The analytical solution for the mathematical model involving energy balance equations of different components of solar air heater is obtained using a MATLAB 8.1. Triple-pass solar air heater with fins exhibits better thermal performance, whereas double-pass solar air heater with fins is economically viable within the opted conditions. The results of the analytical models are in good agreement with experimental findings of earlier researchers.

Keywords Solar air heater · Mathematical model · Triple pass · Longitudinal fins · Thermal performance

List of symbols

A_c	Surface area of the collector (m^2)
A_f	Total surface area of the fins (m^2)
B	Fluid flow channel width (m)
c_p	Specific heat of air at constant pressure (J/kg K)
E	Efficiency increment ratio
G	Air mass flow rate per unit area of collector (kg/m^2 s)
H	Fluid flow channel height (m)
h	Heat transfer coefficient (W/m^2 K)
h_b	Conductive heat transfer coefficient across the insulation (W/m^2 K)
I	Incident solar radiation (W/m^2)
k_s	Thermal conductivity of absorber plate (W/m K)
L	Fluid flow channel length (m)
L_f	Length of the fin (m)
m	Mass flow rate of air (kg/s)
n	Number of the fins
P	Power consumption increment ratio
Q	Useful energy gain of air (W)
t	Thickness of the fin (m)
T	Average temperature (K)
U	Power consumption (W)
W_f	Height of the fin (m)

Greek letters

α	Absorptivity
τ	Transmissivity
ε	Emissivity
η_f	Fin efficiency (%)
η_{th}	Thermal efficiency (%)
σ	Stefan–Boltzmann constant (W/m^2 K^4)

Subscripts

a	Ambient
ab	Absorber plate
b	Back plate
c	Convection
c1	Cover-1
c2	Cover-2
D	Double pass
f	Fluid
f1	Fluid flow-1
f2	Fluid flow-2
f3	Fluid flow-3
i	Inlet
o	Outlet

P. Velmurugan (✉) · R. Kalaivanan
Department of Mechanical Engineering, Annamalai University, Annamalai Nagar 608002, Tamilnadu, India
e-mail: pvsrlme@gmail.com

r Radiation
S Single pass
s Sky
T Triple pass
w Wind

1 Introduction

Solar energy, an alternative energy source, employed to supplement the conventional energy source. The simplest and the efficient way of utilising solar energy is by converting it into thermal energy through solar collector [1]. Solar air heaters are widely employed in low-to-moderate temperature applications, viz. space heating, crop drying, timber seasoning and other industrial applications. The solar air heater occupies an important place among solar heating systems because of the nominal use of materials. The direct use of air as working substance reduces the number of system components required. The lower thermal efficiency owing to inferior heat transfer coefficient is the prime disadvantage in flat-plate absorber solar air heater.

In conventional solar air heater, the area available for heat transfer is lesser than the projected area of the absorber, as it becomes unnecessarily hot, leading to higher heat losses [2]. The convective heat transfer rate in flow channel is augmented by increasing the heat transfer surface area and turbulence inside the channel [3–5]. Though increase in the absorber plate projected area increases the heat transfer rate, pressure drop across the heater increases, and consequently, the power consumption to the air flow through the heater increases [6].

Different modifications are suggested and applied by earlier researchers who employed various design and flow arrangements to improve the heat transfer coefficient between the absorber plate and air. Naphon and Kongtragool [7] applied mathematical models for predicting the heat transfer characteristics and performance of various flow arrangements in a flat-plate solar air heater. Sahu and Bhagoria [8] employed transverse ribs on absorber plate and reported an augmentation in heat transfer coefficient. The performance of single- and double-pass solar air heater with fins and steel wire mesh as absorber was investigated by Omojaro and Aldabbagh [9].

In this work, a novel design of triple-pass solar air heater employing longitudinal fins placed above and below the absorber plate is proposed and studied theoretically. The influence of longitudinal fins in the double-pass solar air heater to enhance the thermal performance of the solar air heater was investigated by several researchers [10–12], whereas the studies on triple pass with fins are limited and are attempted herein. The objective of the present study is (1) to compare the performance of double-pass and triple-pass solar air heaters having fins with that of the conventional solar air heater and (2) to discuss the effect of mass flow rate on thermal efficiency increment and power consumption increment in making the economic consideration.

2 Thermal Modelling of Solar Air Heater

The energy balance analyses at various components of the conventional solar air heater, double-pass solar air heater with fins and triple-pass solar air heater with fins are attempted whose models are shown in Figs. 1, 2 and 3, along with the different heat transfer coefficients at their surfaces. The assumptions made are as follows: (1) heat transfer is steady and one dimensional; (2) heat capacity effects of covers, enclosed air, absorber and back plate are negligible; (3) temperatures of the absorber plate, bottom plate and fluid flow are functions of the flow direction only; (4) there is no air leakage, and flow is turbulent; (5) physical properties of fluid and materials are constant; and (6) outer surface components except the glass cover are thermally insulated as pursued separately by Ramadan et al. [13] and Languri et al. [14].

2.1 Energy Balance Equations for Single-Pass Solar Air Heater Without Fins

The energy balance equations for cover-1, cover-2, fluid flow and absorber plate of the single-pass solar air heater (Fig. 1) assuming $T_{\mathrm{f1}} = (T_{\mathrm{f1i}} + T_{\mathrm{f1o}})/2$ can be written as below

Cover-1

$$\alpha_{\mathrm{c1}} I = h_{\mathrm{w}} (T_{\mathrm{c1}} - T_{\mathrm{a}}) + h_{\mathrm{rc1s}} (T_{\mathrm{c1}} - T_{\mathrm{s}}) + (h_{\mathrm{cc1c2}} + h_{\mathrm{rc1c2}}) (T_{\mathrm{c1}} - T_{\mathrm{c2}}) \quad (1)$$

Cover-2

$$\alpha_{\mathrm{c2}} \tau_{\mathrm{c1}} I = (h_{\mathrm{rc2c1}} + h_{\mathrm{cc2c1}}) (T_{\mathrm{c2}} - T_{\mathrm{c1}}) + h_{\mathrm{rc2ab}} (T_{\mathrm{c2}} - T_{\mathrm{ab}}) + h_{\mathrm{cc2f1}} (T_{\mathrm{c2}} - T_{\mathrm{f1}}) \quad (2)$$

Fluid flow

$$Q_{\mathrm{f1}} = m c_{\mathrm{p}} (T_{\mathrm{f1o}} - T_{\mathrm{f1i}}) = A_{\mathrm{c}} h_{\mathrm{cc2f1}} (T_{\mathrm{c2}} - T_{\mathrm{f1}}) + A_{\mathrm{c}} h_{\mathrm{cabf1}} (T_{\mathrm{ab}} - T_{\mathrm{f1}}) \quad (3)$$

Absorber plate

$$\alpha_{\mathrm{ab}} \tau_{\mathrm{c1}} \tau_{\mathrm{c2}} I = h_{\mathrm{rabc2}} (T_{\mathrm{ab}} - T_{\mathrm{c2}}) + h_{\mathrm{cabf1}} (T_{\mathrm{ab}} - T_{\mathrm{f1}}) + h_{\mathrm{b}} (T_{\mathrm{ab}} - T_{\mathrm{a}}) \quad (4)$$

From Eq. (1), the average temperature of cover-1 is derived as

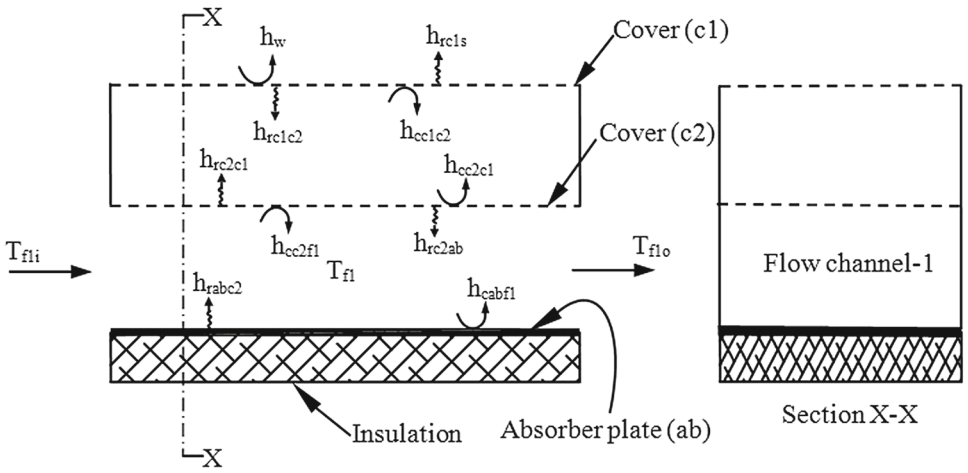

Fig. 1 Single-pass solar air heater without fins

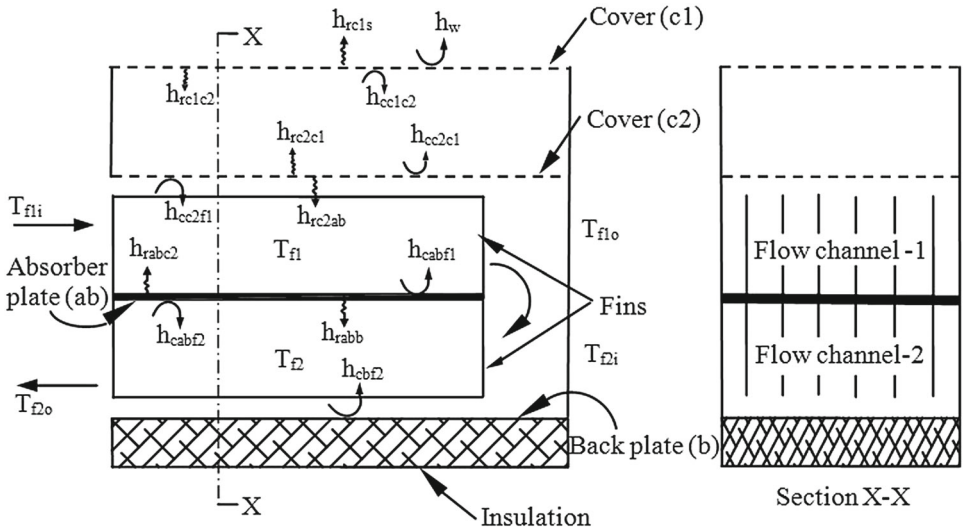

Fig. 2 Double-pass solar air heater with fins

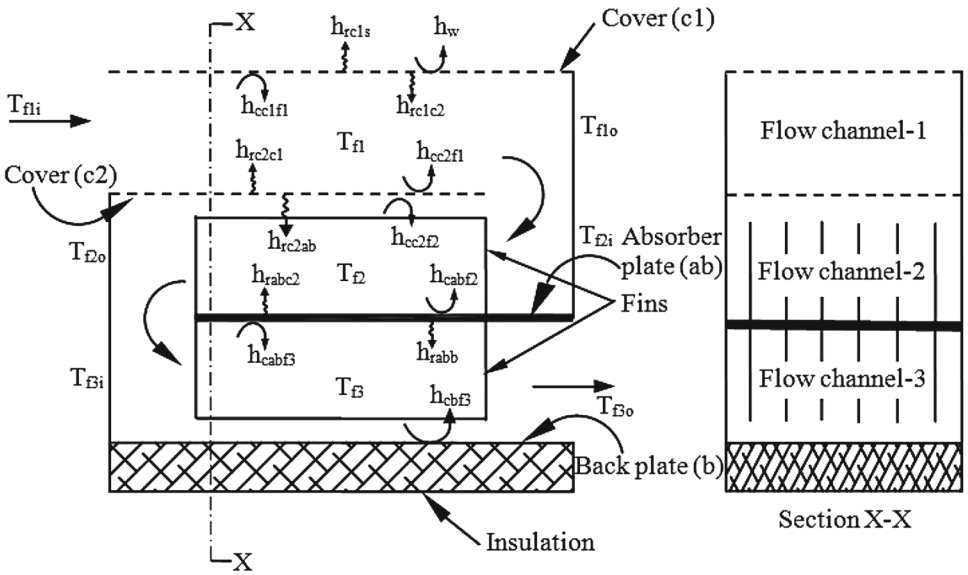

Fig. 3 Triple-pass solar air heater with fins

$$T_{c1} = \frac{\alpha_{c1} I + h_w T_a + h_{rc1s} T_s + (h_{cc1c2} + h_{rc1c2})\, T_{c2}}{h_w + h_{rc1s} + h_{cc1c2} + h_{rc1c2}} \quad (5)$$

The average temperature of cover-2 is determined from Eq. (2) as

$$T_{c2} = \frac{\alpha_{c2}\tau_{c1} I + (h_{rc2c1} + h_{cc2c1})\, T_{c1} + h_{rc2ab} T_{ab} + h_{cc2f1} T_{f1}}{h_{rc2c1} + h_{cc2c1} + h_{rc2ab} + h_{cc2f1}} \quad (6)$$

From Eq. (3), the mean fluid temperature is obtained as

$$T_{f1} = \frac{2Gc_p T_{f1i} + h_{cc2f1} T_{c2} + h_{cabf1} T_{ab}}{2Gc_p + h_{cc2f1} + h_{cabf1}} \quad (7)$$

where G is the air mass flow rate per unit area of collector $= m/A_c$

The average absorber plate temperature obtained from Eq. (4) is given by

$$T_{ab} = \frac{\alpha_{ab}\tau_{c1}\tau_{c2} I + h_{rabc2} T_{c2} + h_{cabf1} T_{f1} + h_b T_a}{h_{rabc2} + h_{cabf1} + h_b} \quad (8)$$

2.2 Energy Balance Equations for Double-Pass Solar Air Heater with Fins

The energy balance equations for cover-1, cover-2, absorber plate, first- and second-pass fluid flows and back plate of the double-pass solar air heater (Fig. 2) assuming $T_{f1} = (T_{f1i} + T_{f1o})/2$ and $T_{f2} = (T_{f2i} + T_{f2o})/2$ are given in Eqs. 9–18.

Cover-1

$$\alpha_{c1} I = h_w (T_{c1} - T_a) + h_{rc1s} (T_{c1} - T_s) + (h_{cc1c2} + h_{rc1c2})(T_{c1} - T_{c2}) \quad (9)$$

Cover-2

$$\alpha_{c2}\tau_{c1} I = (h_{rc2c1} + h_{cc2c1})(T_{c2} - T_{c1}) + h_{rc2ab}(T_{c2} - T_{ab}) + h_{cc2f1}(T_{c2} - T_{f1}) \quad (10)$$

Fluid flow-1

$$Q_{f1} = mc_p (T_{f1o} - T_{f1i}) = h_{cc2f1}(T_{c2} - T_{f1}) + h_{cabf1}\phi (T_{ab} - T_{f1}) \quad (11)$$

where the dimensionless quantity ϕ and fin efficiency η_f are defined with collector surface area A_c and total surface area of fins A_f as

$$\phi = 1 + (A_f/A_c)\,\eta_f \quad (12)$$

$$A_f = 2nW_f L_f \quad (13)$$

$$\eta_f = \tanh(MW_f)/MW_f \quad (14)$$

$$M = \sqrt{2h_{cabf}/k_s t} \quad (15)$$

Absorber plate

$$\alpha_{ab}\tau_{c1}\tau_{c2} I = h_{rabc2}(T_{ab} - T_{c2}) + h_{cabf1}\phi (T_{ab} - T_{f1}) + h_{rabb}(T_{ab} - T_b) + h_{cabf2}\phi (T_{ab} - T_{f2}) \quad (16)$$

Fluid flow-2

$$Q_{f2} = mc_p (T_{f2o} - T_{f2i}) = h_{cabf2}\phi (T_{ab} - T_{f2}) + h_{cbf2}(T_b - T_{f2}) \quad (17)$$

Back plate

$$h_{rabb}(T_{ab} - T_b) = h_{cbf2}(T_b - T_{f2}) + h_b (T_b - T_a) \quad (18)$$

The average temperature of cover-1 from Eq. (9) is given by

$$T_{c1} = \frac{\alpha_{c1} I + h_w T_a + h_{rc1s} T_s + (h_{cc1c2} + h_{rc1c2})\, T_{c2}}{h_w + h_{rc1s} + h_{cc1c2} + h_{rc1c2}} \quad (19)$$

While the average temperature for cover-2 is derived from Eq. (10)

$$T_{c2} = \frac{\alpha_{c2}\tau_{c1} I + (h_{rc2c1} + h_{cc2c1})\, T_{c1} + h_{rc2ab} T_{ab} + h_{cc2f1} T_{f1}}{h_{rc2c1} + h_{cc2c1} + h_{rc2ab} + h_{cc2f1}} \quad (20)$$

From Eq. (11), the mean fluid temperature during first pass is determined as

$$T_{f1} = \frac{2Gc_p T_{f1i} + h_{cc2f1} T_{c2} + h_{cabf1}\phi T_{ab}}{2Gc_p + h_{cc2f1} + h_{cabf1}\phi} \quad (21)$$

The average absorber plate temperature from Eq. (16) is derived as

$$T_{ab} = \frac{\alpha_{ab}\tau_{c1}\tau_{c2} I + h_{rabc2} T_{c2} + h_{cabf1}\phi T_{f1} + h_{rabb} T_b + h_{cabf2}\phi T_{f2}}{h_{rabc2} + h_{cabf1}\phi + h_{rabb} + h_{cabf2}\phi} \quad (22)$$

Similarly, From Eq. (17), the mean fluid temperature during second pass is given by

$$T_{f2} = \frac{2Gc_p T_{f2i} + h_{cabf2}\phi T_{ab} + h_{cbf2} T_b}{2Gc_p + h_{cabf2}\phi + h_{cbf2}} \quad (23)$$

From Eq. (18), the average back plate temperature is estimated as

$$T_b = \frac{h_{rabb} T_{ab} + h_{cbf2} T_{f2} + h_b T_a}{h_{rabb} + h_{cbf2} + h_b} \quad (24)$$

2.3 Energy Balance Equations for Triple-Pass Solar Air Heater with Fins

The energy balance equations for cover-1 and 2, absorber plate, first to third fluid flow and back plate of the triple-pass

solar air heater (Fig. 3) assuming $T_{f1} = (T_{f1i}+T_{f1o})/2$, $T_{f2} = (T_{f2i} + T_{f2o})/2$ and $T_{f3} = (T_{f3i} + T_{f3o})/2$ can be evaluated herein as

Cover-1

$$\alpha_{c1} I = h_w (T_{c1} - T_a) + h_{rc1s} (T_{c1} - T_s) + h_{cc1f1} (T_{c1} - T_{f1}) + h_{rc1c2} (T_{c1} - T_{c2}) \quad (25)$$

Fluid flow-1

$$Q_{f1} = mc_p (T_{f1o} - T_{f1i}) = A_c h_{cc1f1} (T_{c1} - T_{f1}) + A_c h_{cc2f1} (T_{c2} - T_{f1}) \quad (26)$$

Cover-2

$$\alpha_{c2}\tau_{c1} I = h_{cc2f1} (T_{c2} - T_{f1}) + h_{rc2c1} (T_{c2} - T_{c1}) + h_{cc2f2} (T_{c2} - T_{f2}) + h_{rc2ab} (T_{c2} - T_{ab}) \quad (27)$$

Fluid flow-2

$$Q_{f2} = mc_p (T_{f2o} - T_{f2i}) = A_c h_{cc2f2} (T_{c2} - T_{f2}) + A_c h_{cabf2}\phi (T_{ab} - T_{f2}) \quad (28)$$

Absorber plate

$$\alpha_{ab}\tau_{c1}\tau_{c2} I = h_{cabf2}\phi (T_{ab} - T_{f2}) + h_{rabc2} (T_{ab} - T_{c2}) + h_{cabf3}\phi (T_{ab} - T_{f3}) + h_{rabb} (T_{ab} - T_b) \quad (29)$$

Fluid flow-3

$$Q_{f3} = mc_p (T_{3o} - T_{3i}) = A_c h_{cabf3}\phi (T_{ab} - T_{f3}) + A_c h_{cbf3} (T_b - T_{f3}) \quad (30)$$

Back plate

$$h_{rabb} (T_{ab} - T_b) = h_{cbf3} (T_b - T_{f3}) + h_b (T_b - T_a) \quad (31)$$

The average cover temperatures are derived from Eqs. 25, and 27 is given in Eqs. 32 and 33

$$T_{c1} = \frac{\alpha_{c1} I + h_w T_a + h_{rc1s} T_s + h_{cc1f1} T_{f1} + h_{rc1c2} T_{c2}}{h_w + h_{rc1s} + h_{cc1f1} + h_{rc1c2}} \quad (32)$$

$$T_{c2} = \frac{\alpha_{c2}\tau_{c1} I + h_{cc2f1} T_{f1} + h_{rc2c1} T_{c1} + h_{cc2f2} T_{f2} + h_{rc2ab} T_{ab}}{h_{cc2f1} + h_{rc2c1} + h_{cc2f2} + h_{rc2ab}} \quad (33)$$

From Eqs. 26, 28 and 30, the mean fluid temperatures during the first, second and triple pass are given in Eqs. 34–36.

$$T_{f1} = \frac{2Gc_p T_{f1i} + h_{cc1f1} T_{c1} + h_{cc2f1} T_{c2}}{2Gc_p + h_{cc1f1} + h_{cc2f1}} \quad (34)$$

$$T_{f2} = \frac{2Gc_p T_{f2i} + h_{cc2f2} T_{c2} + h_{cabf2}\phi T_{ab}}{2Gc_p + h_{cc2f2} + h_{cabf2}\phi} \quad (35)$$

$$T_{f3} = \frac{2Gc_p T_{f3i} + h_{cabf3}\phi T_{ab} + h_{cbf3} T_b}{2Gc_p + h_{cabf3}\phi + h_{cbf3}} \quad (36)$$

The average absorber plate temperature and back plate temperature of triple-pass solar air heater are determined from Eqs. 29 and 31 as

$$T_{ab} = \frac{\alpha_{ab}\tau_{c1}\tau_{c2} I + h_{cabf2}\phi T_{f2} + h_{rabc2} T_{c2} + h_{cabf3}\phi T_{f3} + h_{rabb} T_b}{h_{cabf2}\phi + h_{rabc2} + h_{cabf3}\phi + h_{rabb}} \quad (37)$$

$$T_b = \frac{h_{rabb} T_{ab} + h_{cbf3} T_{f3} + h_b T_a}{h_{rabb} + h_{cbf3} + h_b} \quad (38)$$

2.4 Heat Transfer Coefficient

The convective heat transfer coefficient (h_w) from the cover-1 to the wind is calculated by the following expression [15] to be valid for a wind speed range $0 \le V_w < 5$ m/s

$$h_w = 5.7 + 3.8 V_w \quad (39)$$

where V_w is wind velocity of the ambient air (m/s).

The radiation heat transfer coefficient (h_{rc1s}) from the cover-1 to sky is obtained as

$$h_{rc1s} = \sigma\varepsilon_{c1} \left(T_{c1}^2 + T_s^2\right) (T_{c1} + T_s) \quad (40)$$

The sky temperature (T_s) for clear-sky condition is estimated by [16]

$$T_s = T_a - 6 \quad (41)$$

The radiative heat transfer coefficients between the absorber plate and both cover-2 (h_{rabc2}) and bottom plate (h_{rabb}) and that between cover-1 and cover-2 (h_{rc1c2}) are calculated by the formula for two infinite parallel plates (i, j):

$$h_{rij} = \sigma \left(T_i + T_j\right) \left(T_i^2 + T_j^2\right) / \left(1/\varepsilon_i + 1/\varepsilon_j - 1\right) \quad (42)$$

where ε_i and ε_j are the emissivities of the two surfaces.

The conduction heat transfer coefficient (h_b) across the insulation (assuming convection and radiation resistances from bottom surface of insulation are negligible) is given by [17]

$$h_b = k_i / t_i \quad (43)$$

where k_i is the thermal conductivity of the insulation (W/m K) and t_i is the thickness of the insulation (m). Due to stagnated air prevailing in parallel plate enclosure between the cover-1 and cover-2, the natural convection heat transfer coefficient (h_{cc1c2}) for single-pass and double-pass is determined by

$$h_{cc1c2} = Nu_{cc1c2} (k/H) \quad (44)$$

where k is the thermal conductivity of air (W/m K) and Nu_{cc1c2} is the Nusselt number for natural convection between the two covers estimated by the following correlation [18]

$$Nu_{cc1c2} = 1 + 1.44\left[1 - \frac{1{,}708}{Ra\cos\theta}\right]^{+} \times\left(1 - \frac{1{,}708\sin(1.8\theta)^{1.6}}{Ra\cos\theta}\right) + \left[\left(\frac{Ra\cos\theta}{5{,}830}\right)^{0.333} - 1\right]^{+} \quad (45)$$

where the '+' symbol in the superscript means that only positive values of the terms in the square brackets are to be used (i.e. use zero if the term is negative). This correlation is valid for $0° \le \theta \le 75°$, $0 < Ra < 10^5$, θ is the angle of inclination of the heater and Ra is the Rayleigh number which is defined as

$$Ra = g\beta\,(T_{c2} - T_{c1})\,H^3/\nu d \quad (46)$$

where β, d, ν are the thermal expansion coefficient (K^{-1}), thermal diffusivity (m^2/s) and kinematic viscosity (m^2/s) of air, g is the acceleration due to gravity (m/s^2).

The forced convection heat transfer coefficients for the fluid moving on the cover-2, on the absorber plate and on the back plate are calculated by

$$h_{cc2f} = h_{cabf} = h_{cbf} = Nu_{cf}\,(k/D_h) \quad (47)$$

where $D_h = 4HB/2\,(H + B)$ is the hydraulic diameter of the fluid flow channel (m) and Nu_{cf} is the Nusselt number for the forced convection in the air flow channel. For the single-, double- and triple-pass heaters, Nu_{cf} can be estimated by the following correlation [19]

$$Nu_{cf} = 0.018\,Re^{0.8}\,Pr^{0.4} \quad (48)$$

where Re is the Reynolds number, defined as

$$Re = 2m/\mu\,(B + H) \quad (49)$$

where μ is the dynamic viscosity of air (kg/m s)

2.5 Thermal Energy Analysis

The useful thermal energy gain (Q_f) by the working fluid is calculated from the following equation [20]

$$Q_f = mc_p\,(T_{fo} - T_{fi}) \quad (50)$$

Thermal energy efficiency (η_{th}) of the heater is obtained from

$$\eta_{th} = Q_f/A_c I \quad (51)$$

2.6 Increment of Thermal Efficiency

The efficiency increment of double-pass solar air heater with fins (E_D) and triple-pass solar air heater with fins (E_T) is defined relative to the single-pass unit without fins as [21]

$$E_D = (\eta_D - \eta_S)/\eta_S \quad (52)$$

$$E_T = (\eta_T - \eta_S)/\eta_S \quad (53)$$

In which η_T, η_D and η_S denote the thermal efficiencies of the triple-pass solar air heater with fins, double- pass solar air heater with fins and single-pass solar air heater without fins.

2.7 Increment of Power Consumption

The necessary instantaneous fan power required for forcing a certain rate of air through the heater is calculated by [13]

$$U = P_{flow}/\eta_{fan}\eta_{motor} \quad (54)$$

where η_{fan} and η_{motor} are fan and motor efficiencies, respectively.

The pumping power P_{flow} is estimated by the following relation [12]

$$P_{flow} = m\Delta P/\rho \quad (55)$$

The pressure drop (ΔP) is determined by

$$\Delta P = \Delta P_{channel} + \Delta P_{bend} \quad (56)$$

The pressure drop ($\Delta P_{channel}$) across the flow channel is estimated as

$$\Delta P_{channel} = 2\rho f L V^2/D_h \quad (57)$$

where f is the friction factor in the channel with fins attached to the absorber plate for turbulent flow and is calculated by [12]

$$f = 0.079\,Re^{-0.25} \quad (58)$$

The pressure drop (ΔP_{bend}) for the 180° close return bend may be calculated as

$$\Delta P_{bend} = K\rho V^2/2 \quad (59)$$

where V is the velocity of flowing air (m/s), K is the coefficient that has the value of 2.2 [22] for the 180° close return bend and ρ is the density of flowing air (kg/m^3).

The power consumption increment of double-pass solar air heater with fins (P_D) and triple-pass solar air heater with fins (P_T) is defined relative to the single-pass solar air heater without fins as [17]

$$P_D = (U_D - U_S)/U_S \quad (60)$$

$$P_T = (U_T - U_S)/U_S \quad (61)$$

where U_T, U_D and U_S represent the power consumption for triple-pass solar air heater with fins, double-pass solar air heater with fins and single-pass solar air heater without fins, respectively.

2.8 Numerical Calculations

In order to evaluate the thermal efficiency of various types of solar air heaters at different mass flow rates, numerical calculations are performed using collector configuration, system properties and operating conditions. The works reporting techniques for determining the cover temperatures (T_{c1} and T_{c2}), absorber plate temperature (T_{ab}), fluid flow temperatures (T_{f1}, T_{f2} and T_{f3}) and back plate temperature (T_b) are sparse. In the present work, the component temperatures above the ambient temperature are initially chosen [13] in order to determine the various heat transfer coefficients using Eqs. (39)–(49), upon which all the above parameters depend on and subsequently the new temperatures of various components are determined by Gauss Seidel iteration method using Eqs. (5)–(8) (for single-pass solar air heater without fins), Eqs. (19)–(24) (for double-pass solar air heater with fins) and Eqs. (32)–(38) (for triple-pass solar air heater with fins). If the new temperatures are larger than 0.01 % from their respective initial values, then the new temperatures will be used as the assumed temperatures for the next iteration and the process is repeated until an optimum new temperature is obtained within ±0.01 % deviation of their respective input values. In order to obtain the thermal efficiency (Eq. 51) numerically, codes are developed in MATLAB 8.1 using following fixed parameters: $t_i = 0.05$ m, $k_i = 0.025$ W/m k, $\varepsilon_{ab} = 0.94$, $\varepsilon_b = 0.94$, $\varepsilon_{c1} = 0.9$, $\varepsilon_{c2} = 0.9$, $\alpha_{ab} = 0.95$, $\alpha_{c1} = 0.06$, $\alpha_{c2} = 0.06$, $\tau_{c1} = 0.84$, $\tau_{c2} = 0.84$, $I = 800$ and 1,000 W/m^2, $m = 0.01, 0.02, 0.03$ and 0.04 kg/s, $L = 2$ m, $\theta = 0°$, $B = 0.46$ m, $H = 0.025$ m, $\sigma = 5.67 \times 10^{-8}$ W/m^2 K^4, $V_w = 1.5$ m/s, $T_a = T_{f1i} = 294$, 300 and 306 K, $t = 0.00095$ m, $n = 17$, $L_f = 1.98$m, $k_s = 50.2$ W/m K, $W_f = 0.025$ m.

3 Results and Discussion

Figures 4 and 5 exhibit the effect of mass flow rate on the outlet temperature and thermal efficiency in single-pass solar air heater without fins, double- and triple-pass solar air heaters with fins at a solar intensity 1,000 W/m^2 and inlet temperature 306 K. The outlet temperature decreases with increase in mass flow rate, and conversely, thermal efficiency increases for all conditions and is consistent with the results of El-Sawi et al. [23]. The increase in flow rate leads to enhancement in heat transfer coefficient between absorber plate and flowing air, resulting in reduced average temperature of the absorber plate and, consequently, higher thermal efficiency [14]. The efficiency of the triple- pass solar air heater with fins is about 8–15 and 3–5 % better than single-pass solar air heater without fins and double-pass solar air heater with fins (Fig. 5) due to increase in heat transfer area and fluid flow conduit.

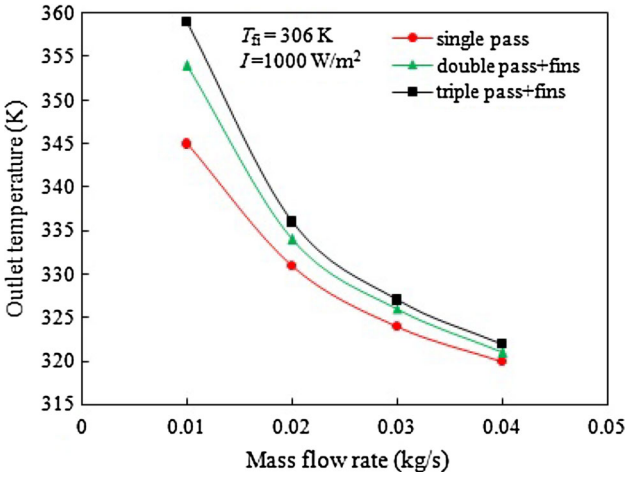

Fig. 4 Predicted variation of outlet temperature with mass flow rate

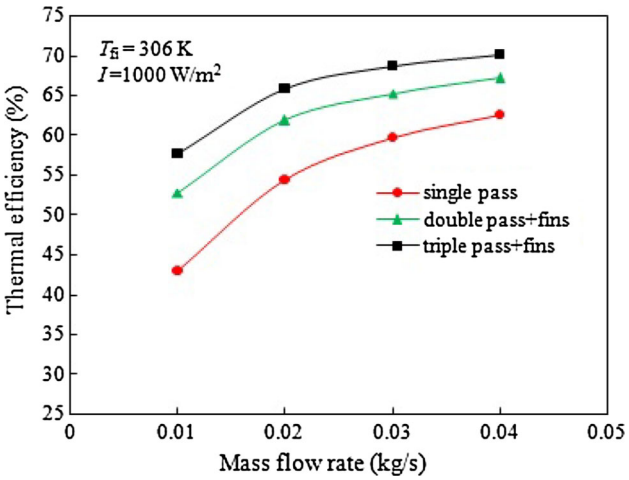

Fig. 5 Predicted variation of thermal efficiency with mass flow rate

In addition, the increase in thermal efficiencies beyond a flow rate of 0.03 kg/s is insignificant (Fig. 5), as the slopes of the thermal efficiency curves decrease, indicating that the overall heat losses nearly reach minimum at higher mass flow rate [12].

From Tables 1 and 2, it is observed that the air outlet temperature and mean absorber plate temperature increase with the air inlet temperature and incident solar radiation, which is consistent with the results of Sopian et al. [24]. The outlet temperatures of triple-pass solar air heater with fins, double-pass solar air heater with fins and single-pass solar air heater without fins increase with incident solar radiation due to increase in absorber plate temperature. As seen from the Tables 1 and 2, the outlet temperature of air and energy efficiency of triple-pass solar air heater with fins (higher enhancement of fluid flow path length and heat transfer area) are higher than that of double-pass solar air heater with fins (moderate enhancement of fluid flow path length and heat transfer area) and also than that of single-

Table 1 Theoretical prediction of solar air heater performance increment for $I = 800\,\mathrm{W/m^2}$

T_{f1i} (K)	Mass flow rate (kg/s)	Single pass			Double pass + fins				Triple pass + fins			
		T_{ab} (K)	T_{f1o} (K)	η_S (%)	T_{ab} (K)	T_{f2o} (K)	η_D (%)	I_D (%)	T_{ab} (K)	T_{f3o} (K)	η_T (%)	I_T (%)
294	0.01	357.68	326.72	44.68	334.73	333.64	54.13	21.15	338.01	337.19	58.97	31.98
	0.02	339.52	314.39	55.71	317.78	316.91	62.54	12.25	319.31	318.31	66.41	19.21
	0.03	329.94	308.81	60.63	310.94	310.05	65.75	8.44	311.83	310.83	68.96	13.73
	0.04	323.95	305.61	63.39	307.21	306.34	67.43	6.37	307.82	306.85	70.23	10.79
300	0.01	362.67	332.31	44.11	339.98	339.29	53.65	21.62	343.57	342.78	58.42	32.44
	0.02	344.95	320.22	55.22	323.64	322.78	62.21	12.65	325.15	324.19	66.06	19.63
	0.03	335.56	314.71	60.23	316.87	315.98	65.49	8.73	317.74	316.76	68.69	14.04
	0.04	329.67	311.54	63.05	313.16	312.31	67.22	6.61	313.76	312.81	69.99	11.01
306	0.01	367.67	337.88	43.54	345.61	344.93	53.16	22.09	349.12	348.37	57.86	32.88
	0.02	350.38	326.04	54.73	329.51	328.65	61.87	13.04	331.01	330.05	65.71	20.06
	0.03	341.18	320.61	59.82	322.79	321.92	65.23	9.04	323.66	322.69	68.41	14.35
	0.04	335.41	317.48	62.71	319.11	318.26	67.01	6.87	319.71	318.77	69.75	11.24

Table 2 Theoretical prediction of solar air heater performance increment for $I = 1{,}000\,\mathrm{W/m^2}$

T_{f1i} (K)	Mass flow rate (kg/s)	Single pass			Double pass + fins				Triple pass + fins			
		T_{ab} (K)	T_{f1o} (K)	η_S (%)	T_{ab} (K)	T_{f2o} (K)	η_D (%)	I_D (%)	T_{ab} (K)	T_{f3o} (K)	η_T (%)	I_T (%)
294	0.01	371.56	334.31	44.03	344.07	343.21	53.76	22.09	348.71	347.77	58.74	33.41
	0.02	350.09	319.36	55.41	323.68	322.61	62.49	12.77	325.68	324.47	66.58	20.15
	0.03	338.52	312.46	60.51	315.18	314.07	65.79	8.72	316.36	315.13	69.24	14.42
	0.04	331.21	308.51	63.36	310.53	309.45	67.52	6.56	311.34	310.15	70.58	11.39
300	0.01	376.37	339.81	43.41	349.61	348.78	53.29	22.75	354.18	353.27	58.19	34.04
	0.02	355.41	325.14	54.93	329.51	328.45	62.17	13.18	331.51	330.32	66.24	20.58
	0.03	344.05	318.34	60.12	321.69	320.03	65.55	9.03	322.26	321.05	68.99	14.75
	0.04	336.86	314.42	63.04	316.47	315.41	67.32	6.78	317.28	316.11	70.36	11.61
306	0.01	381.18	345.29	42.93	355.13	354.34	52.81	23.01	359.64	358.76	57.64	34.26
	0.02	360.71	330.92	54.44	335.33	334.31	61.84	13.59	337.31	336.16	65.89	21.03
	0.03	349.59	324.22	59.71	326.68	325.92	65.29	9.34	328.16	326.97	68.72	15.09
	0.04	342.52	320.34	62.69	322.41	321.35	67.11	7.05	323.91	322.05	70.14	11.88

pass solar air heater without fins (without enhanced path length and heat transfer area) at incident solar radiation of $800\,\mathrm{W/m^2}$ and $1{,}000\,\mathrm{W/m^2}$ considered. Further, increasing of inlet temperature of air and incident solar radiation is not having a significant effect on thermal efficiency and its increment for all conditions (Tables 1, 2). Triple-pass solar air heater with fins shows better performance than single-pass solar air heater without fins and double-pass solar air heater with fins at similar operating condition, while a maximum efficiency increment of 34.26 % is obtained at $I = 1{,}000\,\mathrm{W/m^2}$, $m = 0.01\,\mathrm{kg/s}$ and $T_{fi} = 306\,\mathrm{K}$ with respect to single-pass solar air heater without fins.

The thermal efficiency and power consumption increment in double- and triple-pass solar air heater with fins with respect to single-pass solar air heater without fins at varied mass flow rates is shown in Table 3. When the mass flow rate is increased, thermal efficiency increment decreases, whereas power consumption increment increases for double- and triple-pass solar air heater with fins. An economic analysis of double- and triple-pass solar air heater with fins by considering efficiency increment, power consumption increment, I_D/P_D and I_T/P_T with respect to mass flow rate of air is shown in Table 3 and Fig. 6. The value of I_D/P_D and I_T/P_T decreases with increasing mass flow rate owing to larger power consumption increment, and this fact is consistent with Ho et al. [17] who studied the economic analysis of solar air heater with wire mesh subjected to external flow. The double-pass solar air heater with fins is economical than

Table 3 Effect of mass flow rate of air on efficiency increment and power consumption increment

Mass flow rate (kg/s)	Efficiency increment		Power consumption increment		Efficiency increment / power consumption increment	
	I_D	I_T	P_D	P_T	I_D/P_D	I_T/P_T
0.01	0.2301	0.3426	2.0425	4.0744	0.113	0.084
0.02	0.1359	0.2103	2.1841	4.3683	0.062	0.048
0.03	0.0934	0.1509	2.2847	4.5699	0.041	0.033
0.04	0.0705	0.1188	2.3611	4.7221	0.031	0.025

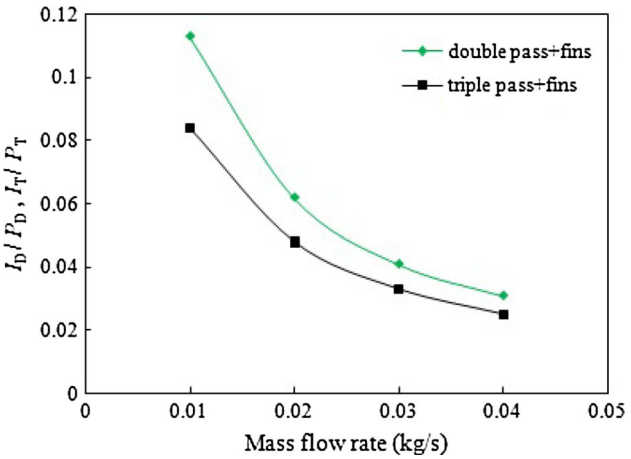

Fig. 6 Predicted variation of I_D/P_D, I_T/P_T ratio with mass flow rate

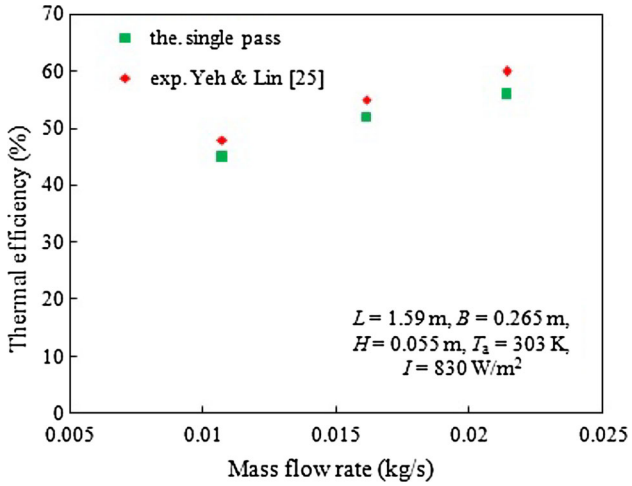

Fig. 7 Comparison of the η_{th} obtained from the model and experimental data for single pass without fins

triple-pass solar air heater with fins due to the higher ratio of useful gain enhancement to power consumption increment at varied mass flow rate of air. The higher power consumption increment due to 180° close return bend and friction in triple-pass conditions supports this behaviour.

In order to validate the developed models, comparisons are performed with the limited available experimental data reported in the literatures. Figure 7 compares the efficiency obtained from mathematical model of single pass without fins with experimental data reported by Yeh and Lin [25], whereas the double-pass with fins experimental data reported by Sebaii et al. [12] are validated with the present model in Fig. 8. It can be seen that the results obtained in mathematical models of single-pass solar air heater without fins and double-pass solar air heater with fins are in reasonable agreement with the experimental data reported by other researchers, giving an average error of 3 and 3.6 %, respectively, for single-pass solar air heater without fins and double-pass solar air heater with fins. The error between experimental and theoretical results is due to uncertainties in the correlations used in calculating various heat transfer coefficients and incident solar radiation on the heater covers. Heat capacities of glass

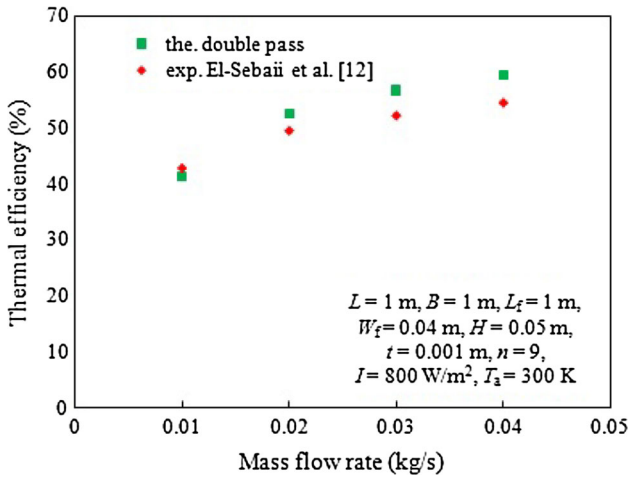

Fig. 8 Comparison of the η_{th} obtained from the model and experimental data for double pass with fins

covers, absorber and back plates, heat losses from edges and sides are not considered in the mathematical analysis, this being another source for error.

4 Conclusion

The mathematical model for predicting the thermal performance of double- and triple-pass solar air heater with fins is presented. The following conclusions are drawn from this analytical study.

1. Mass flow rate is directly proportional to thermal efficiency and conversely with outlet temperature for all conditions.
2. For double- and triple-pass solar air heaters with fins, the variation in inlet temperature and solar intensity has insignificant effect in thermal efficiency increment.
3. Though triple-pass solar heater with fins exhibit higher thermal performance, double-pass solar air heater with fins is economically suitable.
4. Power consumption increment increases with mass flow rate of air for double- and triple-pass solar air heaters.
5. The result of the present analytical study is concurrent with experimental findings of earlier researchers.

References

1. Nandi, S.K.; Hoque, M.N.; Ghosh, H.R.; Chowdhury, R.: Assessment of wind and solar energy resources in Bangladesh. Ar. J. Sci. Eng. **38**(11), 3113–3123 (2013)
2. Yeh, H.M.; Lin, T.T.: Efficiency improvements of flat plate solar air heaters. Energy **21**(7), 435–443 (1996)
3. Lin, W.; Gao, W.; Liu, T.: A parametric study on the thermal performance of cross-corrugated solar air collectors. App. Therm. Eng. **26**, 1043–1053 (2006)
4. Akpinar, E.K.; Koçyiğit, F.: Experimental investigation of thermal performance of solar air heater having different obstacle on absorber plates. Int. Commun. Heat Mass Transf. **37**, 416–421 (2010)
5. Benli, H.: Experimentally derived efficiency and exergy analysis of a new solar air heater having different surface shapes. Renew. Energy **50**, 58–67 (2013)
6. Esen, H.: Experimental energy and exergy analysis of a double flow solar air heater having different obstacles on absorber plates. Build. Environ. **43**, 1046–1054 (2008)
7. Naphon, P.; Kongtragool, B.: Theoretical study on heat transfer characteristics and performance of the flat plate solar air heaters. Int. Commun. Heat Mass Transf. **30**, 1125–1136 (2003)
8. Sahu, M.M.; Bhagoria, J.L.: Augmentation of heat transfer coefficient by using 90° broken transverse ribs on absorber plate of solar air heater. Renew. Energy **30**, 2057–2073 (2005)
9. Omojaro, A.P.; Aldabbagh, L.B.Y.: Experimental performance of single and double pass solar air heater with fins and steel wire mesh as absorber. Appl. Energy **87**, 3759–3765 (2010)
10. Yeh, H.M.; Ho, C.D.; Hou, J.Z.: Collector efficiency of double flow solar air heaters with fins attached. Energy **27**, 715–725 (2002)
11. Karim, M.A.; Hawlader, M.N.A.: Performance investigation of flat plate, v-corrugated and finned air collectors. Energy **31**, 452–470 (2006)
12. El-Sebaii, A.A.; Aboul-Enein, S.; Ramadan, M.R.I.; Shalaby, S.M.; Moharram, B.M.: Thermal performance investigation of double pass-finned plate solar air heater. Appl. Energy **88**, 1727–1739 (2011)
13. Ramadan, M.R.I.; El-Sebaii, A.A.; About Enein, S.; El-Bialy, E.: Thermal Performance of a packed bed double pass solar air heater. Energy **32**, 1524–1535 (2007)
14. Languri, E.M.; Taherian, H.; Hooman, K.; Reisel, J.: Enhanced double-pass solar air heater with and without porous medium. Int. J. Green Energy **8**, 643–654 (2011)
15. Yeh, H.M.: Upward-type flat-plate solar air heaters attached with fins and operated by an internal recycling for improved performance. J. Taiwan Inst. Chem. Eng. **43**, 235–240 (2012)
16. Jafarkazemi, F.; Ahmadifard, E.: Energetic and exergetic evaluation of flat plate solar collector. Renew. Energy **56**, 55–63 (2013)
17. Ho, C.D.; Lin, C.S.; Chuang, Y.C.; Chao, C.C.: Performance improvement of wire mesh packed double-pass solar air heaters with external recycle. Renew. Energy **57**, 479–489 (2013)
18. El-Sebaii, A.A.; Al-Snani, H.: Effect of selective coating on thermal performance of flat plate solar air heaters. Energy **35**, 1820–1828 (2010)
19. Naphon, P.: On the performance and entropy generation of the double-pass solar air heater with longitudinal fins. Renew. Energy **30**, 1345–1357 (2005)
20. Mittal, M.K.; Varshney, L.: Optimal thermohydraulic performance of a wire mesh packed solar air heater. Sol. Energy **80**, 1112–1120 (2006)
21. Ho, C.D.; Chang, H.; Wang, R.C.; Lin, C.S.: Performance improvement of a double-pass solar air heater with fins and baffles under recycle operation. Appl. Energy **100**, 155–163 (2012)
22. Dhiman, P.; Thakur, N.S.; Chauhan, S.R.: Thermal and thermohydraulic performance of counter and parallel flow packed bed solar air heaters. Renew. Energy **46**, 259–268 (2012)
23. El-Sawi, A.M.; Wifi, A.S.; Younan, M.Y.; Elsayed, E.A.; Basily, B.B.: Application of folded sheet metal in flat bed solar air collectors. Appl. Therm. Eng. **30**, 864–871 (2010)
24. Sopian, K.; Alghoul, M.A.; Alfegi, M.E.; Sulaiman, M.Y.; Musa, E.A.: Evaluation of thermal efficiency of double pass solar collector with porous-non porous media. Renew. Energy **34**, 640–645 (2009)
25. Yeh, H.M.; Lin, T.T.: The effect of collector aspect ratio on the collector efficiency of flat plate solar air heaters. Energy **20**, 1041–1047 (1995)